ACS APPLIED MATERIALS & INTERFACES

RESEARCH ARTICLE

www.acsami.org

Electrochemical Monitoring of the Fluorescence Emission of Tetrazine and Bodipy Dyes Using Total Internal Reflection Fluorescence Microscopy Coupled to Electrochemistry

F. Miomandre,* E. Lépicier, S. Munteanu,[$] O. Galangau, J. F. Audibert, R. Méallet-Renault, P. Audebert, and R. B. Pansu*

P.P.S.M., CNRS UMR 8531, PRES UniverSud, Ecole Normale Supérieure de Cachan, 61 Avenue du Président Wilson, 94235 CACHAN Cedex, France

Supporting Information

ABSTRACT: A very sensitive technique where an electrochemical cell is coupled to a total internal reflection fluorescence microscopy setup is described and applied for the first time to the electrochemical monitoring of the fluorescence of organic dyes in solution. It is shown that this setup basically allows both spatial and time resolution for the recorded fluorescence signal as a function of the electrode potential: indeed the variations of the emission intensity are recorded within the diffusion layer for a classical cyclic voltammetry or chronoamperometry experiment inducing the redox conversion of an emissive form into a non emissive one (and conversely). Simultaneously, the variations of the emissive state lifetime are measured to discriminate between a mechanism involving only the conversion into a non emissive form from one involving a quenching between the emitter and the electrogenerated species. The results concerning the investigation of the electrochemical monitoring of the fluorescence properties for two types of original dyes are presented, demonstrating the possibility to switch on and off the emission in a fully reversible way and to investigate in depth the mechanisms associated to this switch.

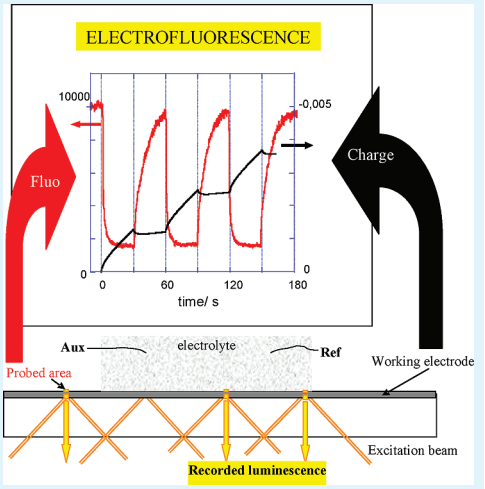

KEYWORDS: TIRF microscopy, fluorescence, electrochemistry, bora-diaza-indacene (Bodipy), tetrazine

INTRODUCTION

The electrochemical monitoring of the fluorescence properties of organic chromophores has known a growing interest during the past few years, with possible applications in the design of new "electrofluorochromic" displays, on the model of the pioneering device made by Kim and Audebert.[1] Bodipy-quinone,[2] Bodipy-ferrocene,[3] ferrocene-diimide,[4,5] and various TTF derivative dyes[6] were recently used as examples to evidence the reversible and stable electrochemical control of the fluorescence properties: the principle of this electrochemically triggered modulation is usually based on the emission quenching by photoinduced electron transfer (PET) in donor−acceptor dyads that is likely to be canceled when the redox state of the donor or acceptor moiety is changed. However, a straightforward fluorescence modulation can also be envisaged with organic dyes provided that their reduction (oxidation) takes place in a reasonable potential range.[7] In all cases where the fluorophore is not grafted on the electrode surface, the detection issue comes from the usually low proportion of fluorophores concerned by the electrochemical switch compared to the bulk concentration, namely, those in the diffusion layer of the electrode. The achievement of a good signal-to-noise ratio depends on the ability to record the fluorescence only in a space very close to the electrode surface, typically a few micrometers. Moreover, the proper understanding of the quenching mechanism requires the record of both the emission intensity and lifetime synchronously with the electrochemical signal. In other words, it would be convenient to record simultaneously the space- and time-resolved fluorescence intensity along with the Coulombic charge, when a potential modulation is applied to a working electrode of an electrochemical cell. We recently proposed a setup coupling epifluorescence microscopy with a three-electrodes electrochemical cell for such a purpose.[8] Besides the coupling of confocal scanning fluorescence microscopy with electrochemistry appeared also very successful to investigate the electrochemical monitoring of the photophysical properties of organic dyes up to the single molecule level.[9] In these two cases, the recorded conversion was not complete, because of residual emission of species remaining in their initial redox state. In this paper, we describe the use of a different configuration of the electrochemistry

Received: October 11, 2010
Accepted: January 5, 2011
Published: February 11, 2011

coupled fluorescence microscopy setup, based on total internal reflection fluorescence (TIRF). Such a configuration allows one to excite only a very thin layer (typically a few hundreds nm) through the evanescent wave propagating in the low refracting index medium, namely the solution in the present case. TIRF is well-known to be a very sensitive technique which can be successfully undertaken to investigate adsorption processes[10] or single molecule detection[11] and was widely developed for biological issues.[12] Nevertheless only a few examples involving the coupling of TIRF microscopy with electrochemical methods can be found in the literature:[13−17] in most cases, the electrochemical signal is used to force the adsorption of the fluorophore onto the electrode surface,[13,14] that is, electrochemistry and TIRF are not actually in situ coupled. When electrochemical control is implemented it is applied to fluorophores grafted on the electrode.[17] In our case, the electrochemical signal is intended to monitor the fluorescence of a dye in solution such that both signals are recorded in situ in a synchronous way. In the present paper, we aim to demonstrate the higher sensitivity of TIRF configuration in the issue of the electrochemical monitoring of the fluorescence of a chromophore located in solution compared to the previous detection mode used for the same purpose.[8] Simultaneous measurements of the variations of fluorescence intensity and lifetime upon the electrochemical signal lead to deep insight into the possible quenching mechanism and this point will be also discussed.

This technique is applied to the investigation of two types of organic fluorophores in solution: tetrazine (Tz)[18] and boradiaza-indacene (Bodipy).[19] These compounds are especially interesting as they are electroactive both in reduction (Tz, Bodipy) and oxidation (Bodipy) with production of ion radical species with various stabilities and also because their photophysical features are now relatively well described in the literature[20−22] while being significantly different. The relation between the electrochemical behaviors of the dyes and their fluorescence modulation features will be discussed in this paper.

EXPERIMENTAL SECTION

Synthesis. The two organic dyes used for these experiments are shown in the Scheme 1.

The synthesis of chloromethoxy-s-tetrazine **1** has been described elsewhere,[20] as well as its main electrochemical and photophysical features.

Synthesis of 4,4-Difluoro-2,6-diethyl-1,3,5,7-tetramethyl-8-perfluorophenyl-4-bora-3a,4a-diaza-s-indacene ***2***. In a three necked round-bottom flask charged with 100 mL of dichloromethane (DCM), were dissolved cryptopyrrole (1.0 g, 8.12 mmol, 2 equiv), perfluorobenzaldehyde (0.796 mg, 4.06 mmol, 1 equiv), and few drops of trifluoroacetic acid (TFA). When the aldehyde was consumed (monitored by TLC), the chloranil oxidation reagent (0.998 mg, 4.06 mmol, 1 equiv) was quickly added. After 5 min, diisopropylethylamine (3.67 g, 28.4 mmol, 7 equiv) was added. After 15 min, boron trifluoride diethyl etherate (6.34 g, 44.6 mmol, 11 equiv) was dissolved. Purification was performed on column chromatography (silica gel, R_f = 0.41) using mixture of petroleum ether and dichloromethane (70/30, v/v) as the eluent. The orange fluorescent fraction was collected and the solvent removal afforded 0.930 mg of **2** as a gold solid (mp = 204−205 °C). Yield: 94%. ^{1}H NMR ($CDCl_3$) δ (ppm): 1.02 (t, 6H, J = 7.56 Hz), 1.51 (s, 6H), 2.34 (q, 4H, J = 7.63 Hz), 2.54 (s, 6H). ^{13}C NMR ($CDCl_3$) δ (ppm): 10.18, 11.35, 12.66, 14.46, 121.21, 130.42, 134.01, 136.65, 156.21. ^{11}B NMR ($CDCl_3$) δ (ppm): −0.27 (t, $^1J_{^{11}B-^{19}F}$ = 31.99 Hz). ^{19}F NMR ($CDCl_3$) δ (ppm): −160.02 (m, 2F), −151.30 (t, 1F, $^3J_{^{19}F-^{19}F}$ = 20.95 Hz), −145.59 (q, 2F, $^1J_{^{19}F\_^{11}B}$= 32.75 Hz), −139.40 (dd, 2F, $^3J_{^{19}F-^{19}F}$ = 23.12 Hz; $^3J_{^{19}F-^{19}F}$ = 7.22 Hz). FTIR: $\nu_{C=C,Ar}$ = 1545 cm^{-1}, $\nu_{C=N}$ = 1497 cm^{-1}. HRMS (ESI): calculated for $C_{23}H_{22}BN_2F_7$ 493.1662, found 493.1679.

Scheme 1. Formulae of the Investigated Compounds

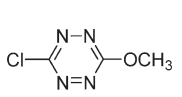

1

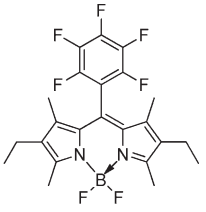

2

Fluorescence Microscopy Coupled to Electrochemistry. The setup used is represented in the Scheme 2. It consists in the association of a classical three electrodes electrochemical cell with an epifluorescence microscope setup.[6] An electrochemical cell containing the analyte solution (concentration 1.5 mM) is stuck on the surface of a microscope glass slide (170 μm thick), which has been coated by a thin platinum layer using a cathodic pulverization apparatus: the estimated metal thickness is 25 nm (from AFM measurements) and its transmittance is ∼10%. This platinum coated glass slide plays the role of the working electrode, while platinum and silver wires dipped into the cell are used, respectively, as counter and pseudoreference electrodes. The area near the electrode surface is probed through the evanescent wave of the excitation laser beam under TIRF conditions; the penetration depth d can be estimated through the equation

$$d = \frac{\lambda}{4\pi} \frac{1}{\sqrt{n_1^2 \sin^2 \theta - n_2^2}} \quad (1)$$

where λ is the excitation wavelength (515 nm), n_1 is the refractive index of glass (1.5), n_2 is the refractive index of the solvent used (1.341 for acetonitrile), and θ is the incident angle.

The pulsed laser source is an Ytterbium TPulse200 from Amplitude Systèmes (Pessac, France) with the following features: 1030 nm (wavelength), 390 fs (pulse width), 10 MHz (pulse frequency), 260 nJ per pulse. The photon energy is doubled to 515 nm by a BBO crystal and injected in the microscope (Nikon, TE2000U) through the epi-illumination port. For TIRF illumination, a 100× objective (APO from Nikon, numerical aperture 1.45) is used. The fluorescence is recorded perpendicularly to the surface in a reverse microscope configuration. The sample is first lit up with a collimated beam in a Köhler configuration. This is done by focusing the laser beam in the back focal plane of the objective with the excitation tube lens (f = 300 mm). The incidence angle of the beam at the sample is then decreased by moving the laser focus in the back focal plane away from the optical axis. The focus is moved by translating the excitation tube lens until the excitation beam is reflected by the sample on the spatial filter pinhole plane.

The fluorescence photons are collected through a side port of the microscope and imaged on the surface of a time and space resolved single photon counting photomultiplier (256 × 256 pixel quadrant anode detector from Europhoton GmbH, Berlin). Data are treated using IgorPro software from Wavemetrics (Oregon).

Lifetime measurements are performed according to time correlating single photon counting: each photon is recorded with its position and arrival time on the photocathode. Fluorescence decays are reconstructed from delay time histograms in the 100 ns period (see Supporting Information for details).

The emission spectra are recorded in two ways. An optical fiber (200 μm in diameter for UV−vis transport) is placed in the image plane of one of the side port of the microscope. The optical fiber selects the light

Scheme 2. (a) Scheme of the Electrochemical Cell (Top) and Platinum Coated Microscope Slide Used for TIRF Measurements (Bottom) and (b) Optical Path for the Excitation and Emitted Beams in the Epifluorescence Set-Up

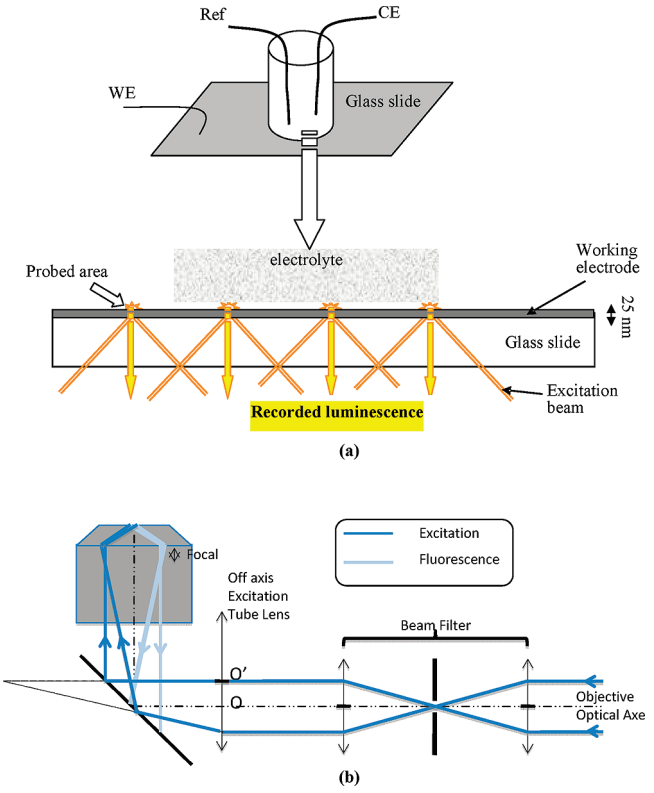

coming from a circle in the image whose diameter is 5% that of the view field. The light is transferred to an Ocean Optics Spectrometer (USB2000+ UV−vis). Fluorescence spectra, as well as transmission intensities, are acquired with the SpectraSuite software. Alternatively a slit is placed on the image plane of the side port of the microscope that is imaged by the quadrant anode detector. In the Fourier space, a grating is placed that makes a spectrum imaged on the quadrant anode detector. This allows us to make video of the nanosecond time-resolved fluorescence spectra.

RESULTS AND DISCUSSION

Tetrazine. First, we have checked that the application of an electrochemical modulation between two values of potential inducing no redox change for the fluorophore had actually no influence on the recorded intensity, thus eliminating possible artifacts due to, for example, bleaching phenomena (see Supporting Information). Figure 1 displays the simultaneous variations of fluorescence intensity and redox charge recorded for a staircase potential signal between 0 and −0.9 V (3 cycles of 30 s) applied to a solution of **1** in acetonitrile. These two potential values correspond respectively to the absence of reduction and the complete reduction of chloromethoxytetrazine **1** at the electrode surface (see the corresponding CV in figure 2A). One can see that the fluorescence intensity is actually modulated by the applied potential. Such a modulation had been already measured in the wide field transmission mode,[8] but with a much smaller amplitude than in the present case. Here the modulation is fully reversible, both from the fluorescence and electrochemistry points of view, once the redox charge is corrected from natural

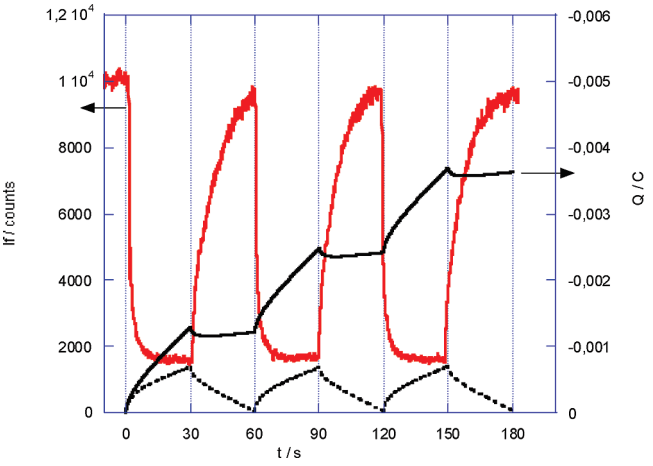

Figure 1. Simultaneous record of fluorescence intensity (left scale) and redox charge (right scale) for a solution of **1** in acetonitrile submitted to potential staircase signals between 0 and −0.9 V (3 cycles of 60 s). The dashed line is the redox charge after subtraction of the background current.

diffusion effects.[23] The initial value of the fluorescence signal is recovered on the time period. The origin of the fluorescence intensity in the "off" state will be discussed below.

The influence of the applied potential is shown in Figure 2: the lower value of the fluorescence intensity decreases when the electrode potential becomes more negative (Figure 2B); the trend is confirmed by comparing the variation of the electrode concentration in neutral tetrazine predicted by Nernst law with the one of the fluorescence intensity (Figure 2C). The slight shift between both curves can be assigned to the fact that fluorescence is not recorded strictly at the interface but in an area close to it. The thickness of this area corresponds to the penetration depth of the evanescent wave associated with the excitation beam and can be estimated to a few hundreds of nanometers.

Figure 3A shows the variation of the fluorescence intensity with the time period of the potential signal. For the two longer periods, the initial fluorescence intensity is recovered while the shortest time is not sufficient to reach back the initial value. One can check that the extreme intensity values are not modified when the potential is stepped between the same values. Looking closer to the shape of the variations of the fluorescence intensity, one can notice that the decrease upon reduction is always steeper than the increase upon reoxidation.

In first approximation, one could assume that the fluorescence intensity is proportional to the concentration in neutral tetrazine, which is in turn related to the Coulombic charge. When looking more closely at the reoxidation step, the fluorescence intensity I_f varies linearly with the reoxidation charge (corrected from natural convection effects), which in turn varies linearly with $\theta = ((\tau)^{1/2} - (t)^{1/2} + (t-\tau)^{1/2})$, where τ is the reversal time.[24] This linearity between I_f and θ is evidenced in figure 3B. This variation is characteristic of a diffusional process for the electroactive species, and the result is that the rate of the fluorescence recovery is limited by the diffusion rate of the neutral form at the interface vicinity. This process is not valid to explain the variation of fluorescence upon reduction, since I_f does not vary in a linear way with the square root of time, as the Coulombic charge (corrected from natural convection effects) does. Thus an additional process must contribute to the fluorescence decay as discussed further.

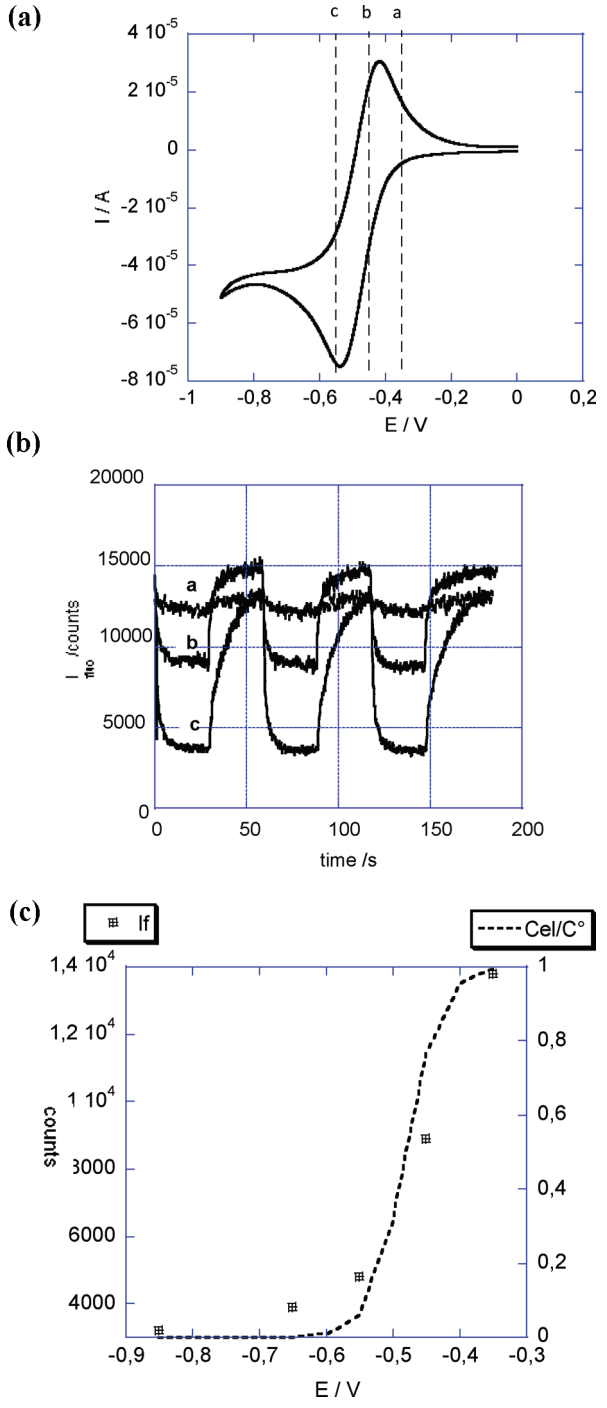

Figure 2. (A) CV of **1** in acetonitrile (scan rate = 50 mV/s) recorded in the TIRF cell. Potential values (a−c used for curves B) are reported on the graph. (B) Variation of fluorescence intensity for double potential steps (30 s each) from 0 to the following values (V): (A) −0.35, (B) −0.45, and (C) −0.55. (C) Fluorescence intensity in the reduced state (squares) and normalized concentration of **1** at the electrode surface according to Nernst equation (dashed line) as functions of final potential.

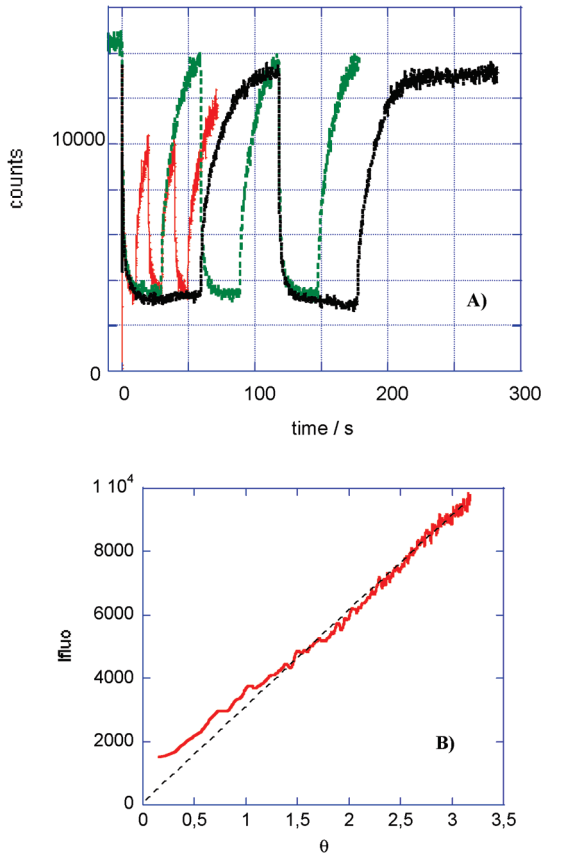

Figure 3. (A) Variation of the fluorescence intensity with time of compound **1** in acetonitrile for 3 periods of the potential staircase signal: 10, 30, and 60 s. Potential is stepped between 0 and −0.8 V. (B) Variation of the fluorescence intensity with $\theta = ((\tau)^{1/2} - (t)^{1/2} + (t - \tau)^{1/2})$ for the first reoxidation potential step (from −0.85 to 0 V).

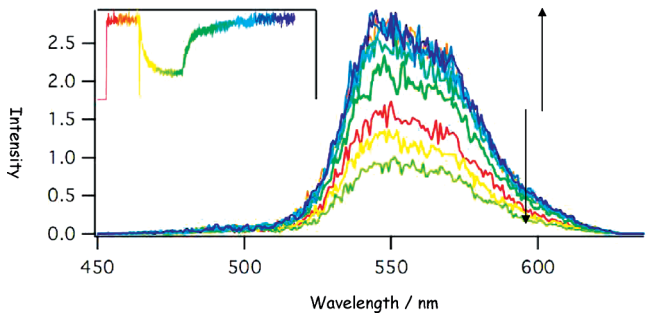

Figure 4. Variation of the emission spectrum of **1** recorded simultaneously to the fluorescence intensity (inset) for a double potential step between 0 and −0.8 V. The various colors correspond to the various times in the inset.

Besides, it would be interesting to ascribe the nonzero value for the intensity in the reduced state, either to incomplete electrochemical conversion or to possible fluorescence of the anion radical of tetrazine. Such a discrimination was also intriguing in the case of the confocal microscopy configuration.[9] The evidence for correct assignment was given by the compared rate of photon collection upon reduction and oxidation. In the present case, the clue is provided by the analysis of lifetime and spectral variation associated to the electrochemical signal. Figure 4 shows the emission spectra recorded at several times of the double step potential. In the spectral region of interest, only one broad emission band corresponding to the neutral tetrazine can be seen: the intensity of this band gradually decreases and increases upon reduction and oxidation, without any changes in the shape

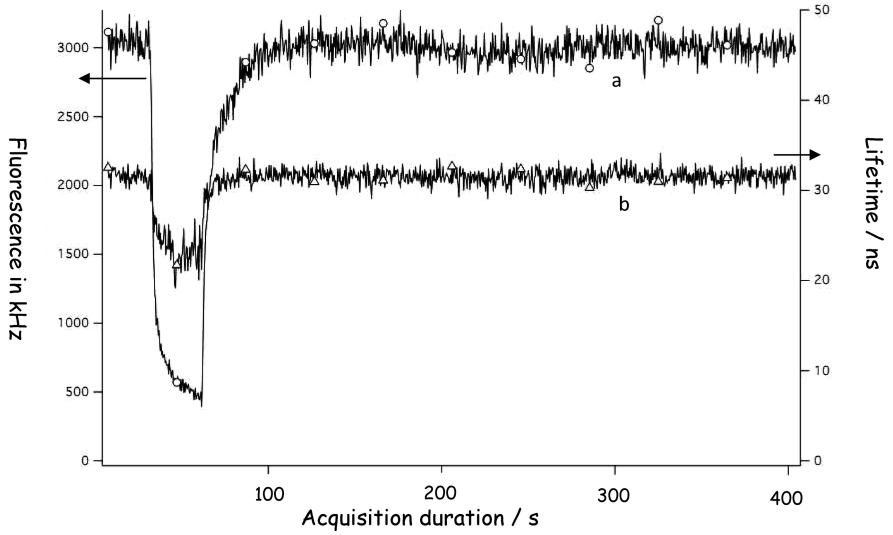

Figure 5. Evolution of the fluorescence lifetime (b, right scale) along with the fluorescence intensity (a, left scale) for a double step potential between 0 and −0.85 V.

nor appearance of new bands. This result is consistent with the presence of only one fluorophore (the neutral tetrazine) and thus the background intensity is not the result of a weaker emission coming from the anion radical but rather to either incomplete redox conversion, as already mentioned by Ackermann[9] or to residual fluorescence coming from out of the diffusion layer. Another possibility in the case of tetrazines could arise from the regeneration of the neutral form through oxidation of the anion radical by residual oxygen on long time scales: this assumption is corroborated by the lower backward currents actually observed for CV recorded at the end of the electrofluorochromic experiments compared to the one recorded just after argon bubbling. This could explain the much higher fluorescence level in the "off" state observed for tetrazines compared to Bodipy (see below). However there is no influence from the fluorophore concentration, which makes unlikely any contribution from energy transfer between fluorophores during the emission lifetime, despite the especially long value of this latter for compound **1**.

Figure 5 displays the variation of the fluorescence lifetime associated to the double step potential. This curve is obtained by computing the average delay of the fluorescence photons with respect to the laser pulse at several times of the electrochemical signal.[25] A weak but significant modulation of the lifetime with the time (and thus with the potential) is evidenced. This means that the gradual disappearance of the fluorophore upon electrochemical reduction is not the only explanation of the overall intensity decay: there is also a contribution due to quenching phenomena. This quenching is not due to residual oxygen gas since the fluorescence quantum yield of tetrazine derivatives is not sensitive to oxygen and in the present case, the same behavior was observed for the freshly degassed solution. Moreover the modulated signal clearly involves the electrochemical reaction in the quenching process. It is likely that the electrogenerated species (anion radical) contributes to the quenching either by electron transfer (the anion radical is able to reduce the Tz excited state) or energy transfer (if the main absorption band of the anion radical overlaps the emission band of the tetrazine). As mentioned before, this lifetime modulation does not depend on the emission wavelength thus confirming the assumption of a single fluorophore in the investigated range (450−700 nm). This quenching process is the key factor in the dissymmetry observed between the fluorescence drop and recovery stages, since this is more pronounced as the applied potential is more negative. The faster the anion radical is produced the steeper the fluorescence drop is while the recovery appears slower. Thus it is likely that the electrogenerated species takes part to the quenching mechanism and thus contribute to the rate of the intensity drop. Looking at the amplitude of the lifetime variation, one can assess the quenching rate assuming a dynamic quenching following Stern−Volmer equation:[26]

$$\frac{1}{\tau} = \frac{1}{\tau_0} + k_Q[Q] \qquad (2)$$

where [Q] is the quencher concentration, k_Q is the quenching rate, and τ_0 is the fluorescence lifetime in absence of quenching. Here the quencher is the electrogenerated species, thus the lifetime modulation amplitude $\Delta\tau = \tau_0 - \tau$ can be expressed as a function of the concentration of electrogenerated anion radical by rearranging eq 2 into

$$\frac{\Delta\tau}{\tau} = k_Q \tau_0 [Tz^{\bullet -}] \qquad (3)$$

If the concentration of anion radical is taken equal to its electrode surface value, namely the bulk concentration of neutral Tz (1.5 mM), one can estimate the quenching rate to be $k_Q \cong 10^{10}$ L mol^{-1} s^{-1}, which is precisely the order of magnitude for diffusion limited bimolecular rate constants. Thus the amplitude of the lifetime modulation is compatible with a dynamic quenching taking place according to the following equation:

$$Tz^* + Tz^{\bullet -} \rightarrow Tz^{\bullet -} + Tz$$

Indeed, as the quenching reaction regenerates the quencher, it is likely that it operates at the maximal diffusion limited rate constant calculated above, despite the diffusion of the electrogenerated anion radical.

If one assumes that the anion radical concentration follows the same variation with time as the Coulombic charge,[27] then the plot of $\Delta\tau/\tau = f(t^{1/2})$ should be linear at least for the initial times where natural convection can be neglected (see Supporting Information). Despite the noise caused by the difficulty to

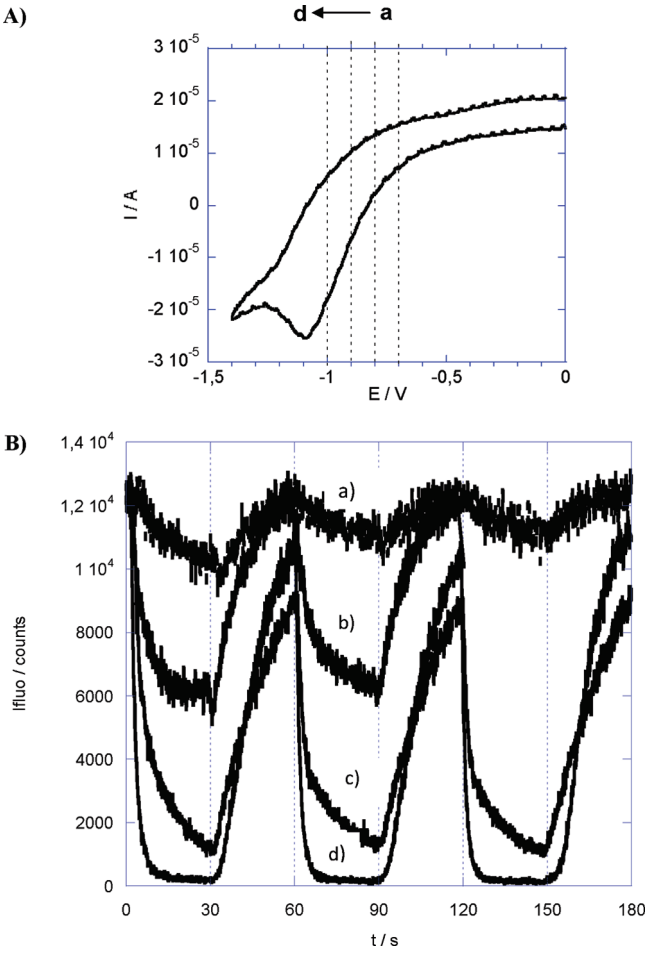

Figure 6. (A) CV of compound **2** in acetonitrile (50 mV/s) in TIRF cell. (B) Variation of the fluorescence intensity for compound **2** corresponding to double potential steps from 0 to the following values (V): (a) −0.7, (b) −0.8, (c) −0.9, and (d) −1.

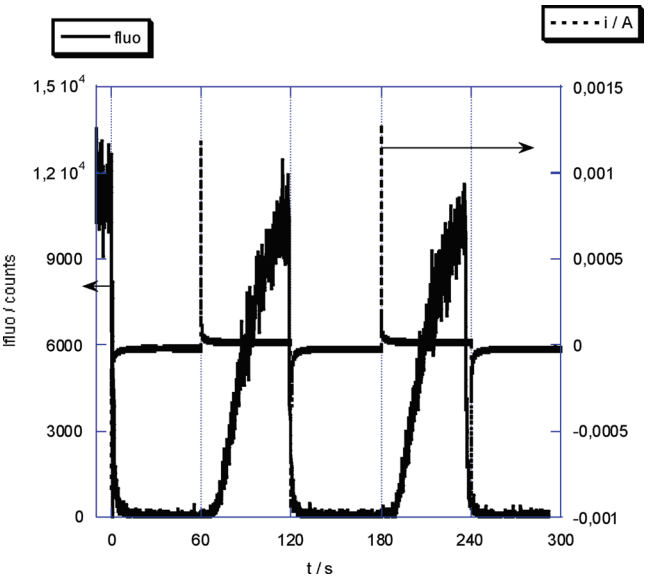

Figure 7. Variation of fluorescence intensity (left scale) and current (right scale) for compound **2** in acetronitrile when applying double potential steps from 0 and −1.1 V (2.5 cycles of 120 s each are shown).

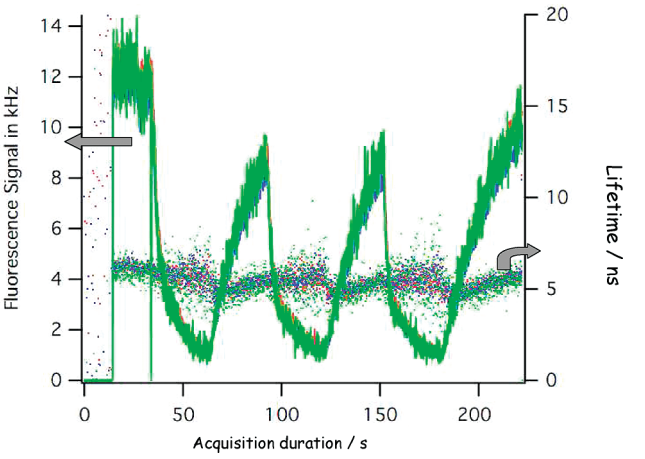

Figure 8. Variations of fluorescence intensity (left scale) and lifetime (right scale) of **2** in acetonitrile for double step potentials between 0 and −0.9 V (60 s each). The blue, green and red curves are associated with emission wavelengths (540, 570, and 620 nm, respectively).

measure lifetimes as the fluorescence signal collapses, the linear fit is acceptable. The same trend is also observed for the plot of $1/I_F = f(t^{1/2})$, in agreement with the Stern−Volmer equation coupled to a diffusion limited concentration of quencher in the probed area.

Bodipy. Figure 6 shows the variation of fluorescence intensity upon reduction−reoxidation of compound **2**. As shown in the CV (Figure 6A), Bodipy **2** bears a non reversible reduction in these experimental conditions, with the electrogenerated anion radical consumed by a following chemical reaction. Figure 6B displays the fluorescence modulation as a function of the applied potential in double step chronoamperometry: it is clear that the switch off is very efficient for **2** as it starts even for potentials corresponding to the foot of the redox wave, and is complete for potentials below the reduction peak. Figure 7 shows the modulation for potential corresponding to full electrochemical conversion. While switch off is very fast and complete (fluorescence intensity is almost zero in the reduced state), switch on upon reoxidation is very slow, with a final intensity still below the initial one after times as long as 60 s, contrariwise to the Tz case where the initial intensity was recovered after 30 s (see Figure 3).Indeed the absence of electrogenerated anion radical in the diffusion layer upon reoxidation leads to a delay in the fluorescence recovery. When looking at the lifetime variation corresponding to the reduction at half peak potential (figure 8), one can notice a much lower amplitude (∼10%) compared to the Tz case. Once again the absence of electrogenerated species in the diffusion layer prevents the quenching mechanism to occur simultaneously to the fluorescence decrease due to the consumption of the emissive form (neutral). In that case, the fluorescence decay is mainly due to the disappearance of the emissive form. The much lower fluorescence level reached in the reduced state compared to the Tz case could be related to a more efficient conversion but lower background fluorescence resulting from irradiation outside of the diffusion layer can not be ruled out since lower excitation energy is required to generate the Bodipy fluorescence.

A similar behavior is observed for the oxidation of **2**, showing that the fluorescence can be monitored also in the reverse way: a fast decrease of fluorescence intensity is associated with oxidation

of **2** with a final value gradually decreasing when the applied potential becomes more positive. The fluorescence recovery is much slower upon backward reduction especially when the oxidation has been performed at the highest potential values (see. Supporting Information). So it seems that the different electrochemical behaviors observed for both dyes leads to various features in the fluorescence modulation, especially as far as the kinetics is concerned. Additional investigations are in progress to quantify the relation between electrochemical and fluorescence kinetics, as well as the role of dye concentration and incidence angle.

CONCLUSION

We have demonstrated the efficiency and high sensitivity of TIRF microscopy coupled to electrochemistry in the monitoring of fluorescence properties for two organic dyes in solution. Reversible switch of the fluorescence intensity with high amplitude modulation can be obtained upon potential step signals in the time range of a few seconds. The amplitude of the modulation is directly related to the potential limit value and dependent on the reversible character of the electrochemical reaction. A synchronous modulation of the fluorescence lifetime with the intensity is recorded in the case of tetrazine, evidencing a quenching process, which is ascribed to electron transfer reactions between the excited neutral fluorophore and the electrogenerated anion radical. For Bodipy, a very fast fluorescence drop is observed for reduction and oxidation without lifetime modulation due to unstable electrogenerated species in the experimental conditions. All these promising results are likely to be extended to other systems like redox functionalized or multicomponent fluorophores, in the aim to develop multistate "electrofluorochromic" devices.

ASSOCIATED CONTENT

Supporting Information. Fluorescence decays of **1** and details on the numerical fits for calculation of lifetimes. Analysis of the chronocoulograms of **1**, electrofluorescence curves of **1** for a lower concentration, and CV and electrofluorescence curves for oxidation of **2**. This material is available free of charge via the Internet at http://pubs.acs.org.

AUTHOR INFORMATION

Corresponding Author

*E-mail: mioman@ppsm.ens-cachan.fr (F.M.); pansu@ppsm.ens-cachan.fr (R.B.P).

Present Addresses

$LECA, ESPCI, Paris.

ACKNOWLEDGMENT

The authors are very grateful to A. Brosseau (PPSM) for the deposition of the platinum layers and the thickness control by AFM. Dr G. Clavier is also acknowledged for fruitful discussion.

REFERENCES

(1) Kim, Y.; Kim, E.; Clavier, G.; Audebert, P. *Chem. Commun.* **2006**, 3612–3614.

(2) Benniston, A. C.; Copley, G.; Elliot, K. J.; Harrington, R. W.; Clegg, W. *Eur. J. Org. Chem.* **2008**, 2705.

(3) Rao, M.; Pavan Kumar, K.; Ravikanth, M. *J. Organomet. Chem.* **2010**, *695*, 863.

(4) Zhang, R. L.; Wang, Z. L.; Wu, Y. S.; Fu, H. B.; Yao, J. N. *Org. Lett.* **2008**, *10*, 3065–3068.

(5) Sun, L.; Tian, H. *Tetrahedron Lett.* **2006**, *47*, 9227–9231.

(6) Canevet, D.; Sallé, M.; Zhang, G.; Zhang, D. Q.; Zhu, D. B. *Chem. Commun.* **2009**, *17*, 2225.

(7) Dias, M.; Hudhomme, P.; Levillain, E.; Perrin, L.; Sahin, Y.; Sauvage, F. X.; Wartelle, C. *Electrochem. Commun.* **2004**, *6*, 325–330.

(8) Miomandre, F.; Meallet-Renault, R.; Vachon, J. J.; Pansu, R. B.; Audebert, P. *Chem. Commun.* **2008**, *16*, 1913.

(9) Lei, C.; Hu, D.; Ackerman, E. J. *Chem. Commun.* **2008**, 5490–5492.

(10) Tang, Y. J.; Chen, Y.; Yao, M. N.; Zou, Z. X.; Han, G. B.; Li, Y. Q. *J. Fluoresc.* **2008**, *18*, 261–267.

(11) Ruckstuhl, T.; Rankl, M.; Seeger, S. *Manipulation Anal. Biomol., Cells Tissues* **2003**, *4962*, 126–134.

(12) Trache, A.; Meininger, G. A. *Current Protocols in Microbiology*; John Wiley & Sons, 2008, Chapter 2, Unit 2A.2.1−2A.2.22.

(13) Asanov, A. N.; Wilson, W. W.; Odham, P. B. *Anal. Chem.* **1998**, *70*, 1156–1163.

(14) Li, L.; Tian, X. Z.; Zou, G. Z.; Shi, Z. K.; Zhang, X. L.; Jin, W. R. *Anal. Chem.* **2008**, *80*, 3999–4006.

(15) Amatore, C.; Arbault, S.; Chen, Y.; Crozatier, C.; Lemaitre, F.; Verchier, Y. *Angew. Chem., Int. Ed.* **2006**, *45*, 4000–4003.

(16) Loete, F.; Vuillemin, B.; Oltra, R.; Chaumont, D.; Bourillot, E. *Electrochem. Commun.* **2006**, *8*, 1016–1020.

(17) Salverda, T. M.; Patil, A. V.; Mizzon, G.; Kuznetsova, S.; Zauner, G.; Akkilic, N.; Canters, G. W.; Davis, J. J.; Heering, H. A.; Aartsma, T. J. *Angew. Chem., Int. Ed.* **2010**, *49*, 5776–5779.

(18) Audebert, P.; Clavier, G. *Chem. Rev.* **2010**, *110*, 3299.

(19) Loudet, A.; Burgess, K. *Chem. Rev.* **2007**, *107*, 4891.

(20) Audebert, P.; Miomandre, F.; Clavier, G.; Vernières, M. C.; Badré, S.; Méallet-Renault, R. *Chem.—Eur. J.* **2005**, *11*, 5667–5673.

(21) Golovkova, T. A.; Kozlov, D. V.; Neckers, D. C. *J. Org. Chem.* **2005**, *70*, 5545.

(22) Trieflinger, C.; Rurack, K.; Daub, J. *Angew. Chem., Int. Ed.* **2005**, *44*, 2288.

(23) For the timescales used in these chronocoulometric measurements natural convection leads to a steady-state current, that is, an additional charge varying linearly with time (see Supporting Information for details)

(24) Bard, A. J.; Faulkner *Electrochemical Methods: Fundamentals and Applications*, 2nd ed.; Wiley: New York, 2000.

(25) The real fluorescence lifetime of **1** in the experimental conditions was estimated to 127 ns by fitting the decays (see Supporting Information). Lifetime values measured during the electrochemical switch are underestimated because integrating dark current. Nevertheless this does not influence the relative variations.

(26) Valeur, B. *Molecular Fluorescence: Principles and Applications*; Wiley: New York, 2001.

(27) This is reasonable since the fluorescence is measured in a fixed volume close to the electrode surface, theoretically equal to the electrode area x the penetration depth ($A \times d$). Thus the electrogenerated species concentration in this volume should be proportional to the injected charge.